Analyst

PAPER

View Article Online
View Journal

Cite this: DOI: 10.1039/d5an00491h

PAM-free activation of CRISPR/Cas12a *via* semi-nested asymmetric RPA: highly specific detection of HPV16 dsDNA†

Xiaozhi Zou,[a] Tao Gu,[a] Xuheng Li,[a] Liyuan Deng,[a] Shuyu Zhu,[a] Jiangbo Dong,[a] Fei Deng,[b] Changjun Hou *[a] and Danqun Huo*[a]

Received 3rd May 2025,
Accepted 14th July 2025

DOI: 10.1039/d5an00491h

rsc.li/analyst

Early and accurate detection of HPV16 nucleic acids is therefore critical for the effective screening, diagnosis, and prevention of cervical cancer. Although CRISPR/Cas12a-based molecular diagnostics offer a rapid and sensitive approach for HPV16 detection, their application to double-stranded DNA (dsDNA) targets remains constrained by two major limitations: the strict requirement for a protospacer adjacent motif (PAM) site and the insufficient specificity of current amplification strategies, which can lead to off-target amplification and false-positive results. To address these challenges, we developed a semi-nested asymmetric recombinase polymerase amplification (SNA-RPA) method combined with CRISPR/Cas12a for the detection of HPV16 dsDNA. This strategy employs a semi-nested primer design to significantly enhance target sequence specificity during amplification, while asymmetric primer ratios promote the efficient generation of single-stranded DNA (ssDNA) that directly activates Cas12a without the need for a PAM site. Using this approach, we achieved rapid and highly specific detection of HPV16 dsDNA, with a limit of detection as low as 18 aM. Beyond achieving PAM-free detection, our method also substantially improves amplification fidelity, offering a promising solution for precise and reliable HPV diagnostics and cervical cancer screening.

1 Introduction

Cervical cancer ranks fourth in the global cancer mortality rate among women.[1,2] In the majority of cervical cancer cases (84%), persistent human papillomavirus (HPV) infection that promotes the integration of the viral genome into the cellular genome is critical in the development of cervical cancer.[3,4] Among the more than 200 HPV genotypes that have been identified, 15 high-risk HPV (HR-HPV) types have been shown to be associated with the progression of cervical cancer as well as precancerous lesions.[5] Among them, HPV16, which is uniquely oncogenic, is responsible for half of all cervical cancer cases.[6,7] Therefore, the development of a rapid test for HPV16 is essential for early screening and timely prevention of most cases of cervical cancer.

Currently, cervical cytology and HPV testing are the primary methods for cervical cancer screening.[8] However, cervical cytology, which relies on the microscopic examination of cellular morphology, suffers from notable limitations, including operational variability in sample collection and preservation, as well as subjective interpretation by pathologists, leading to a false-negative rate of 20–25%.[9] To overcome these limitations, molecular diagnostics targeting HPV nucleic acids have emerged as a promising alternative. By directly detecting the presence of viral genetic material with high specificity and sensitivity, HPV nucleic acid tests offer a more objective, reproducible, and early means of identifying high-risk infections, thereby enhancing the effectiveness of cervical cancer screening programs.[10,11] The current gold standard for HPV nucleic acid detection is polymerase chain reaction (PCR)-based testing.[12] Although PCR provides high sensitivity and specificity, its requirement for skilled personnel, expensive thermal cyclers, and precise experimental conditions has increased operational complexity and infrastructure costs.[13] Moreover, the need for multiple temperature shifts during amplification prolongs assay time, making PCR less suitable for point-of-care or field-deployable diagnostics.[14] Therefore, the development of new nucleic acid detection methods is still required to overcome these limitations and further improve the efficiency and practicality of HPV screening.

[a]*Key Laboratory for Biological Science and Technology of Ministry of Education, Bioengineering College of Chongqing University, Chongqing 400044, PR China. E-mail: houcj@cqu.edu.cn, huodq@cqu.edu.cn; Fax: +86 23 6510 2507; Tel: +86 23 6511 2673*

[b]*Graduate School of Biomedical Engineering, Faculty of Engineering, University of New South Wales, Sydney 2052, Australia. E-mail: fei.deng@unsw.edu.au*

† Electronic supplementary information (ESI) available. See DOI: https://doi.org/10.1039/d5an00491h

In this context, numerous isothermal amplification techniques have been developed,[15–19] among which recombinase polymerase amplification (RPA) stands out due to its ease of operation and short reaction time, making it particularly well-suited for rapid, on-site detection. To further enhance the specificity and sensitivity of RPA-based detection, the CRISPR/Cas12a system has been widely incorporated as a terminal signal transduction module, enabling efficient conversion of nucleic acid concentration information into detectable fluorescent signals.[20–22] Cas12a exhibits both *cis*- and *trans*-cleavage activities upon recognition of double-stranded DNA (dsDNA) bearing a protospacer adjacent motif (PAM) sequence (5′-TTTN-3′).[23,24] When oriented towards dsDNA, Cas12a forms a complex with crRNA and localizes to the target DNA near the PAM, which activates the *cis*- and *trans*-cleavage activities of Cas12a, ultimately causing amplification of the signal.[25] However, Cas12a recognition of single-stranded DNA (ssDNA) does not require a PAM site.[26,27] This dependency on PAM sequences poses a significant limitation: target dsDNA molecules lacking the necessary PAM cannot be directly detected by Cas12a, restricting its broader application.

To address this issue, several strategies have been developed. Li *et al.* incorporated additional PAM sequences blocked within hairpin structures, where target binding opened the hairpin, enabling amplification *via* hybridization chain reaction to form a functional PAM and activate Cas12a.[28] Zhou *et al.* introduced a 5′-phosphate modification on one RPA primer, allowing Lambda exonuclease to generate ssDNA from RPA amplicons for Cas12a activation.[29] Meng *et al.* engineered LAMP primers to yield dsDNA with enzymatic cleavage sites, producing ssDNA through digestion and strand displacement, bypassing PAM restrictions.[30] However, these methods rely on complex primer designs, costly enzymes, or specialized modifications, limiting their universality and cost-effectiveness for broad application.

Therefore, there remains a need for a simplified, cost-effective method to achieve PAM-independent nucleic acid detection. Asymmetric amplification utilizes unequal pairs of primers to generate a large amount of ssDNA without additional enzymes and modifications, which solves the problem of PAM site restriction in Cas12a assay.[31] However, the efficiency of ssDNA production with conventional asymmetric amplification is relatively low. To further enhance both the specificity and yield of target sequences, semi-nested amplification employs nested primers to selectively enrich and amplify the target region, significantly improving the amplification specificity and efficiency.[32] Thus, by combining asymmetric amplification with semi-nested amplification, it is possible to achieve rapid, highly specific conversion of double-stranded DNA (dsDNA) to ssDNA along with effective target sequence amplification to achieve PAM free detection by Cas12a.

In this study, we developed a semi-nested asymmetric recombinase polymerase amplification (SNA-RPA) strategy that efficiently amplifies target sequences by leveraging the concentration differences among three primers, generating a large amount of single-stranded DNA (ssDNA) without the need for additional enzymatic treatment. This ssDNA subsequently activates the CRISPR/Cas12a system for sensitive fluorescence-based detection. Our method enables the direct detection of HPV16 double-stranded DNA (dsDNA) without PAM site constraints, achieving a detection limit as low as 18 aM within 70 minutes. By integrating semi-nested amplification and asymmetric RPA, the system significantly improves detection specificity and sensitivity while expanding the range of detectable HPV16 dsDNA fragments for Cas12a, offering a rapid, simple, and highly effective approach for PAM-free nucleic acid diagnostics.

2 Materials and methods

2.1 Experimental reagents and DNA sequences

All reagents (Table S1†) and DNA sequences (Table S2†) are shown with information in the Appendix.

2.2 Establishment of the SNA-RPA -CRISPR/Cas12a fluorescence detection method

The ERA (KS101) nucleic acid amplification kit was purchased from GenDx Biotech Co. (Suzhou, China). The SNA-RPA system consisted of 1 μL of 1 μM reverse primer (R), RPA lyophilized powder, 20 μL of solubilizer, 20 μL of DNase/RNase-free water, 2 μL of activator, and 4 μL of target nucleic acid (the control was 4 μL nuclease-free water), which were mixed well and divided into the top and bottom of four PCR tubes. Then, 1 μL of 0.75 μM forward outer primer (F1) was added at the top and 1 μL of 25 μM forward inner primer (F2) was added at the bottom, respectively. After incubation at 37 °C for 5 min, centrifugation and mixing, the mixture was incubated again at 37 °C for 15 min. After that, the CRISPR/Cas12a system was configured according to Table S1,† and 4 μL of the RPA product was transferred to the configured CRISPR/Cas12a system, mixed, and then incubated at 37 °C for 50 min, and then placed in an FL970 fluorescence spectrophotometer for fluorescence acquisition.

2.3 Gel electrophoresis analysis

To assess the feasibility of the experiment, we first used 10% polyacrylamide gel (configuration method in Table S2†) and 2% agarose gel (0.6 g agarose powder added to 30 mL of 1× TBE buffer) for analysis. Next, the samples were first reacted in the PCR instrument at 56 °C for 5 min, and then mixed with 6× loading buffer at a volume ratio of 5 : 1, and 10 μL was added to the wells. After that, electrophoresis conditions for both were: reaction in 1× TBE buffer at 90 V for 120 min. Once electrophoresis was completed, the gel was submerged in GelRed for 12 min. Finally, the electropherograms were captured using Azure Biosystems C10 (USA) software.

2.4 Optimization of conditions based on SNA-RPA-CRISPR/Cas12a fluorescence assay

In order to obtain more ssDNA, we optimized the reaction system. In this system, the yield of ssDNA is closely related to

the concentration of primers and the time of the RPA reaction. Therefore, we investigated the concentration of F1 and F2, hoping that F1 and R can produce more dsDNA for F2 to produce more ssDNA. Next, we tested different concentrations of F1 (0.25 μM, 0.5 μM, 0.75 μM, 1 μM, and 2 μM) and F2 (10 μM, 15 μM, 20 μM, 25 μM, and 30 μM). Then, we optimized the RPA reaction time by dividing it into pre-centrifugation amplification time, which was set to 0 min, 5 min, 10 min, 15 min, and 20 min, and post-centrifugation amplification time, which was set to 5 min, 10 min, 15 min, 20 min, and 25 min. After that, to obtain greater fluorescence intensity, we optimized the cutting time of the CRISPR/Cas12a system, which was set to 20 min, 30 min, 40 min, 50 min, and 60 min.

2.5 Exploration of the performance of a fluorescence assay based on SNA-RPA-CRISPR/Cas12a

To explore the sensitivity, specificity and reproducibility of this method, we first diluted HPV16 dsDNA from 1 nM to 100 aM in a 10-fold gradient and utilized this method to amplify samples at different concentrations. The obtained fluorescence values were used to calculate linear regression. To assess the specificity of this method, HPV16 dsDNA and four random sequences were detected using this method. In addition to assessing the reproducibility of the method, five independent replicate experiments were performed to calculate RSD values to evaluate the reproducibility of the method.

2.6 Serum spiking experiment

A 10% human normal serum sample was used to dilute the target to different concentrations (10 fM, 1 pM, and 10 pM) to simulate a complex biological environment. Afterward, the reaction of SNA-RPA-CRISPR/Cas12a was performed, fluorescence intensity was collected, and the theoretical concentration was calculated by linear regression analysis to compare with the actual concentration.

3 Results and discussion

3.1 Principles of HPV16 detection by SNA-RPA-CRISPR/Cas12a

Here, we developed the SNA-RPA technique to overcome the PAM site limitation of CRISPR/Cas12a and realize the rapid and sensitive detection of HPV16 (Scheme 1). First, we designed three primers based on the sequence of HPV16, in which the forward outer primer (F1) and reverse primer (R) amplification sequences contain the region amplified by the forward inner primer (F2) and R. In this system, the R concentration is less than the sum of the concentrations of all the former primers. The forward primer content is excess R. Next, as illustrated in Scheme 1, when the target was present, F1 and F2 were amplified by RPA with R in the cap and at the bottom of the tube, respectively. After 5 min of amplification, the reaction mixture was centrifuged. F1 and F2 continued to amplify with R until R was consumed. At this stage, the excess F2 and F1 primers amplified a large amount of ssDNA using previously amplified dsDNA as a template. This enabled the activation of Cas12a without recognizing the PAM site to generate *trans*-cutting activity, which cleaved the F–Q reporter to obtain fluorescence. In this process, F2 used the F1 and R amplified dsDNA as a template to further improve the specificity of the assay and reduce the false-positive problem of non-specific amplification; meanwhile, the semi-nested asymmetric RPA in two consecutive amplifications also improved the amount of ssDNA, which enhanced the sensitivity of the assay. In addition, the CRISPR/Cas12a system recognized ssDNA and cleaved the fluorescent reporter F–Q to produce

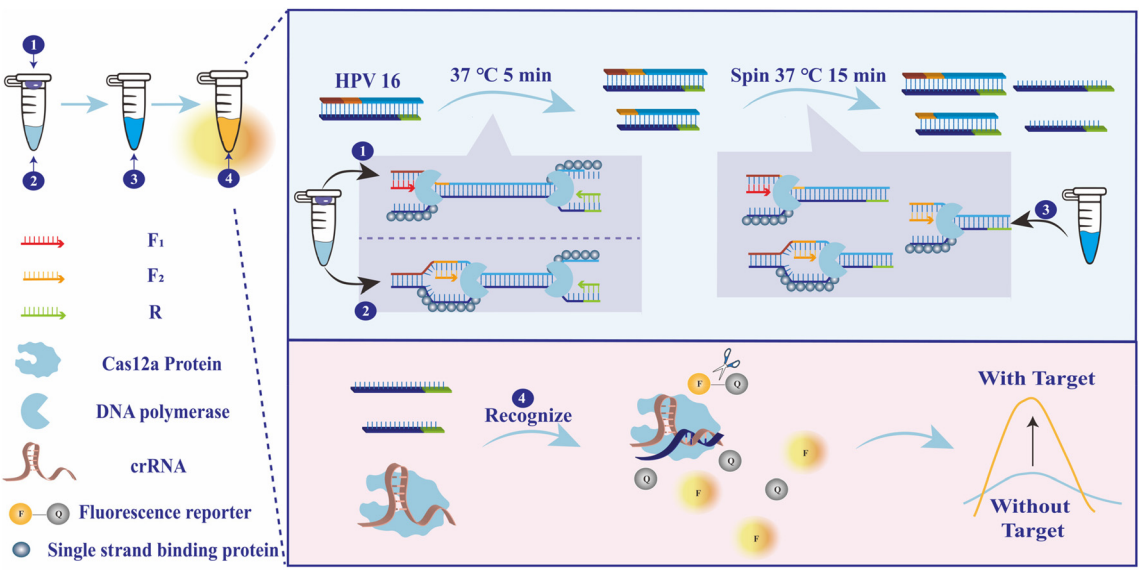

Scheme 1 Schematic diagram of HPV16 dsDNA detection based on SNA-RPA.

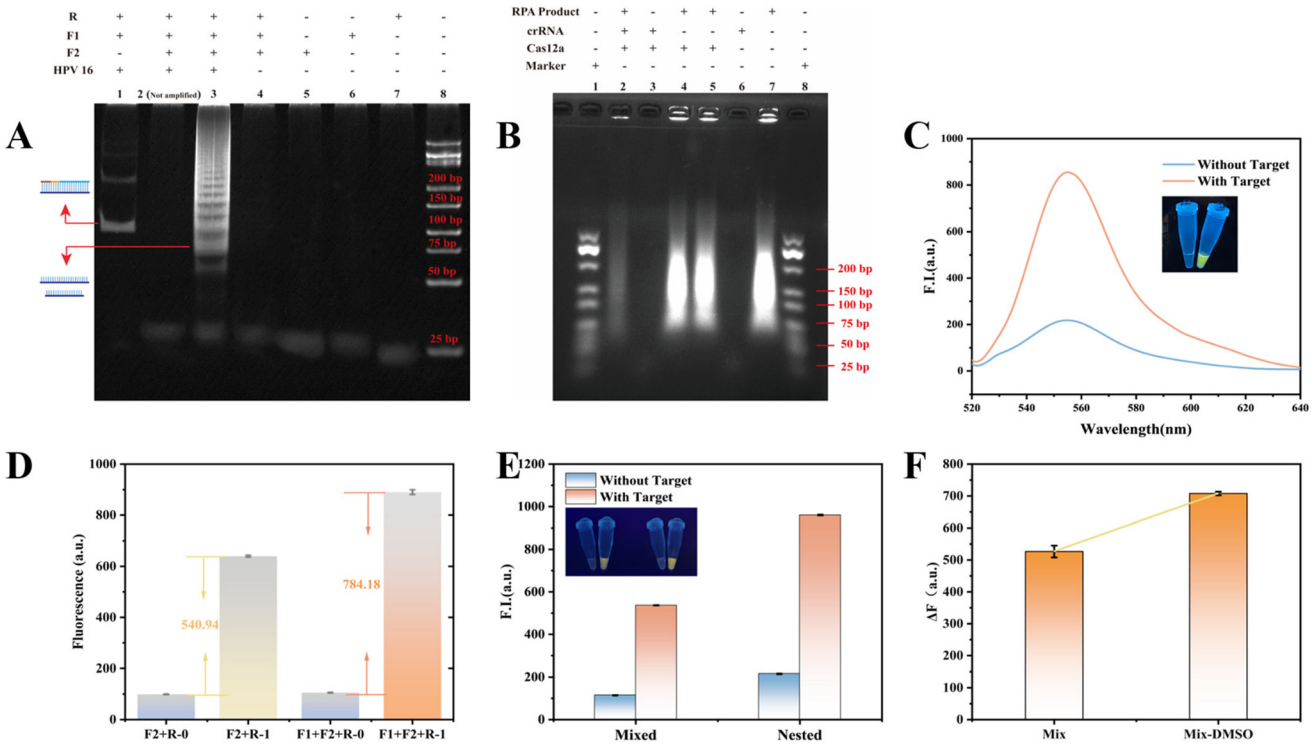

Fig. 1 Feasibility demonstration of SNA-RPA for HPV16 dsDNA detection. (A) Polyacrylamide electropherogram of SNA-RPA; (B) CRISPR/Cas12a cleavage confirmation agarose gel plot; (C) fluorescence intensity of HPV16 dsDNA measured using this assay: blank group and control group; (D) comparison between conventional asymmetric RPA and nested asymmetric RPA (negative *vs.* positive group); (E) fluorescence intensity of SNA-RPA using different mixing methods; (F) comparison of mixed RPA and mixed RPA added to DMSO. All the experiments were conducted in triplicate and graphs are presented as mean ± standard deviation (SD).

strong fluorescence, which further improves the sensitivity and specificity of this method. This approach resulted in a 60% increase in ssDNA productivity compared to traditional asymmetric RPA (Fig. 1D). In conclusion, SNA-RPA-CRISPR/Cas12a can directly convert dsDNA to ssDNA without enzyme changes. This effect can solve the problem of the PAM site and finally improve the range of Cas12a's selection of HPV16 dsDNA target fragments.

3.2 The feasibility of SNA-RPA-CRISPR/Cas12a

In order to assess the feasibility of SNA-RPA, we explored this assay by PAGE and gel electrophoresis. As shown in Fig. 1A, it was first confirmed that the primers (R, F1, and F2) were all 30 bp (lanes 5, 6, and 7). When the target was not present, the three primers could not pair with each other for self-amplification under the amplification conditions, proving that the design of the three primer sequences would not interfere with the experimental results (lane 4). When the target is present and the only primers present are F1 and R, with the amplification of RPA, the product is dsDNA with 98 bp in lane 1. With the participation of F2, after R was consumed, the excess forward primer was able to produce a large amount of ssDNA using the previously amplified dsDNA as a template (lane 3). In addition, other bands of different sizes appeared in lane 3. We have analysed ssDNA self-binding by NUPAK and found that two ssDNA form partial double-stranded structures. On this basis, DNA polymerase can use these complexes as templates and continue to extend them to generate non-target products larger than 98 bp. The above results indicated that HPV16 dsDNA was able to successfully initiate the SNA-RPA reaction with the participation of three primers. To verify whether the obtained ssDNA could be recognized by crRNA and thus activate the *trans*-cutting activity of Cas12a, we performed gel electrophoresis analysis of the CRISPR/Cas12a reaction process and found that the *trans*-cutting activity of Cas12a was activated only in the presence of the RPA product, crRNA, and Cas12a at the same time (Fig. 1B lane 2). At the same time, we also verified the feasibility of the Cas12a sensing system. Fig. S1† shows that strong fluorescence is produced only in the presence of the target, crRNA, and Cas12a.

To further test the feasibility of this method, we performed fluorescence spectroscopy experiments. As shown in Fig. 1C, strong fluorescence is produced only in the presence of HPV16 dsDNA, while the fluorescence of the blank group is low. This result indicates that the HPV16 dsDNA amplified with the three primers by the SNA-RPA reaction to produce a large amount of ssDNA, which can activate the *trans*-cleavage activity of Cas12a without the need for the PAM site and release fluorescent signals. Conversely, in the absence of the target, the RPA reaction with Cas12a cleavage could not be triggered.

Meanwhile, SNA-RPA did not increase background signals despite the additional primer and demonstrated higher ssDNA acquisition efficiency than conventional asymmetric RPA (Fig. 1D). In addition, we investigated the mixing method to obtain greater amplification efficiency (Fig. 1E). We found that the efficiency of RPA amplification by centrifugation and mixing of F1 and F2 with R in the cap and at the bottom of tubes, respectively, was better than that of direct mixing of the three primers for RPA amplification. This may be due to the presence of inter-primer interference or competition in the direct mixing system. Therefore, we added DMSO, which can reduce primer dimer formation, to the mixed system to indirectly verify the above conjecture. As shown in Fig. 1F, the efficiency of the mixed amplification set was significantly improved after the addition of DMSO, so it can be shown that separate amplification can reduce more dimers, resulting in a higher fluorescence signal response. Overall, the SNA-RPA assay was able to achieve superior amplification efficiency of ssDNA than conventional asymmetric RPA, proving that this assay can subsequently improve the sensitivity for ssDNA detection by CRISPR/Cas12a.

3.3 The optimization of SNA-RPA experimental conditions

In order to achieve optimal detection efficiency, we systematically optimized five important parameters in our experiments (F1 concentration, F2 concentration, F1 and F2 separated RPA amplification time, RPA amplification time after centrifugal mixing of both amplification systems, and CRISPR/Cas12a cutting time). The F1 and R amplification sequence contains the region amplified by F2 with R. Therefore, F2 can use the dsDNA produced by F1 and R as a template for secondary amplification. Meanwhile, due to the exhaustion of the R primer in SNA-RPA, the remaining F1 and F2 can obtain a large amount of ssDNA using the amplified dsDNA as a template. Thus, the concentration of F1 and F2 played a key role in cyclic amplification. As shown in Fig. 2A and B, ΔF (experimental group fluorescence minus control group fluorescence) gradually increases with the increase of the concentration of F1 and F2, and the signal intensity is maximum when the concentration of F1 is 0.75 μM and the concentration of F2 is 25 μM, which indicates that SNA-RPA amplified the ssDNA most efficiently. In addition, compared with the mixing RPA, SNA-RPA amplified more efficiently using the same material and within the same time. To further improve the efficiency of SNA-RPA to obtain a large amount of ssDNA, we optimized the time of F1 and F2 separated RPA amplification and RPA amplification time after centrifugal mixing of both amplification systems. As shown in Fig. 2C and D, the maximum fluorescence value is reached by F1 and F2 separated RPA amplification for 5 min, and RPA amplification for 15 min after centrifugation and mixing of both amplification systems. Finally, the signal output intensity of the assay is not only related to ssDNA yield, but also to CRISPR/Cas12a cleavage time. As shown in Fig. 2E, the fluorescence intensity increases with the increase of CRISPR/Cas12a cleavage time and reaches the maximum value at 50 min, indicating that 50 min was the optimal reaction time. In conclusion, the optimized conditions include: 0.75 μM F1 primer, 25 μM F2 primer, 5 min primer-separated RPA amplification, 15 min RPA amplification after centrifugal mixing of both amplification systems, and 50 min CRISPR/Cas12a cutting. Ultimately, a high signal-to-noise ratio fluorescence signal output is achieved.

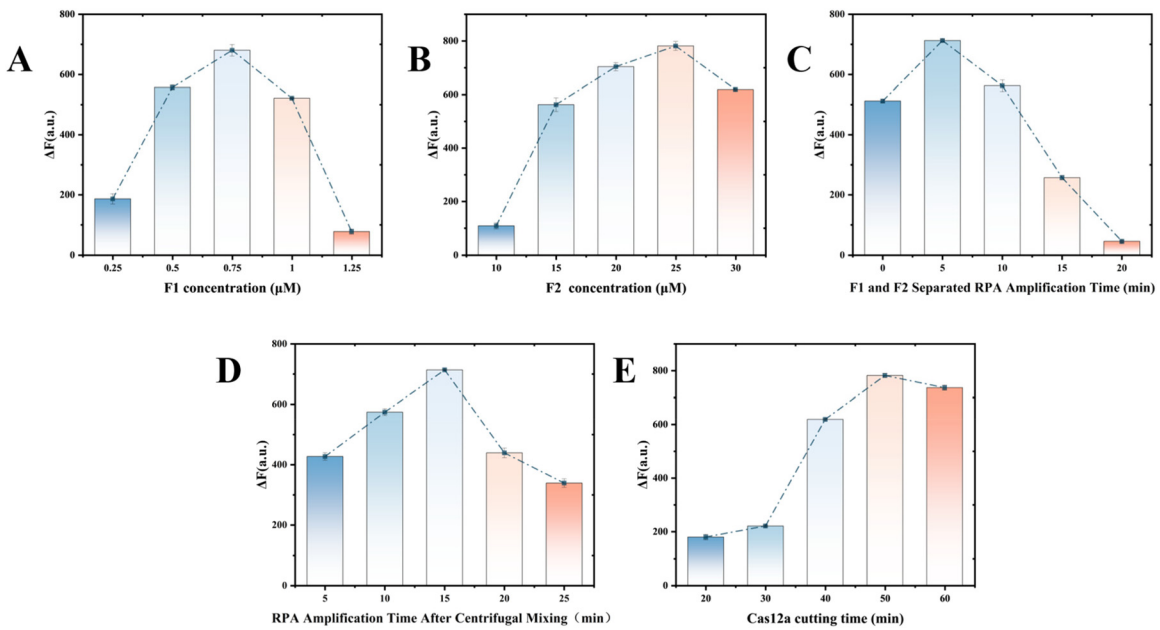

Fig. 2 Optimization of F1 concentration (A), F2 concentration (B), F1 and F2 separated RPA amplification time (C), RPA amplification time after centrifugal mixing of both amplification systems (D), and CRISPR/Cas12a shear time (E). All the experiments were conducted in triplicate and graphs are presented as mean ± standard deviation (SD).

3.4 The performance of SNA-RPA for HPV16 detection

To explore the detection performance of this method, we measured the changes in fluorescence intensity arising from different concentrations of HPV16 dsDNA under optimal detection conditions. Fig. 3A shows the fluorescence curves generated by different concentrations of HPV16 dsDNA in the range of 100 aM–1 nM. As the concentration of HPV16 dsDNA increased, the gradual increase of ssDNA activated more Cas12a, resulting in a concomitant increase in fluorescence intensity (Fig. 3B). As shown in Fig. 3C, there was a good linear relationship between the ΔF (the fluorescence of the experimental group minus the fluorescence of the control group) value and the logarithm of HPV16 dsDNA concentration in the experimental group, with a linear equation of $\Delta F = 104.621\lg(c/10\ \text{aM}) - 43.446$ ($R^2 = 0.997$), where c represents the concentration of HPV16 dsDNA. After calculation, the limit of detection (LOD) of this method is 18 aM, and compared with other detection methods (Table S3†), this method has a lower detection limit and a wider detection range. The excellent performance of this method is mainly attributed to the following reasons: the design of the three primers in SNA-RPA and the utilization of the concentration difference of the primers, which enables the excess primers to use the amplified double strand as a template to increase the yield of ssDNA, while improving the specificity of the assay. In addition, the combination of the CRISPR/Cas12a system further increases the specificity of the assay. Single-stranded DNA needs to be specifically recognized by crRNA to activate Cas12a activity, which ensures the precise recognition of the target. We also tested HPV16 dsDNA (100 pM–1 fM) using the golden standard qPCR (Fig. 3D). As the target concentration increased, the qPCR cycle threshold (C_t) decreased and the ΔC_t (the value of the control group minus the value of the experimental group) showed a strong linear relationship, which was $\Delta C_t = 3.863\lg(C/1\ \text{fM}) - 2.737$ ($R^2 = 0.999$), with an LOD of 134 aM. Finally, our assay can achieve sensitivity that is 0.87 order of magnitude better than that of the gold standard qPCR (Fig. 3E), proving its high potential for low concentration HPV16 ssDNA detection.

3.5 Investigation of the reproducibility and repeatability of the SNA-RPA assay

To further investigate the selectivity and reproducibility of this assay. First, we selected the HPV18 sequence as well as three random sequences as interfering sequences, which were at a concentration of 100 pM. As shown in Fig. 4A and Fig. S2,† strong fluorescence is observed only in the presence of HPV16 dsDNA, and the rest of the four random sequences with the blank group show low fluorescence intensity. After that, we tested five independent groups of samples of HPV16 dsDNA to explore the reproducibility of this assay (Fig. 4B and Fig. S3†), and it was found that the relative standard deviation (RSD) of the net fluorescence values calculated between the five independent groups of samples was 2.12%, which was less than 5%, indicating that the SNA-RPA method has good stability.

3.6 Serum spiking detection

To assess the practicality of the SNA-RPA-CRISPR/Cas12a assay, we performed a series of spiking recovery experiments

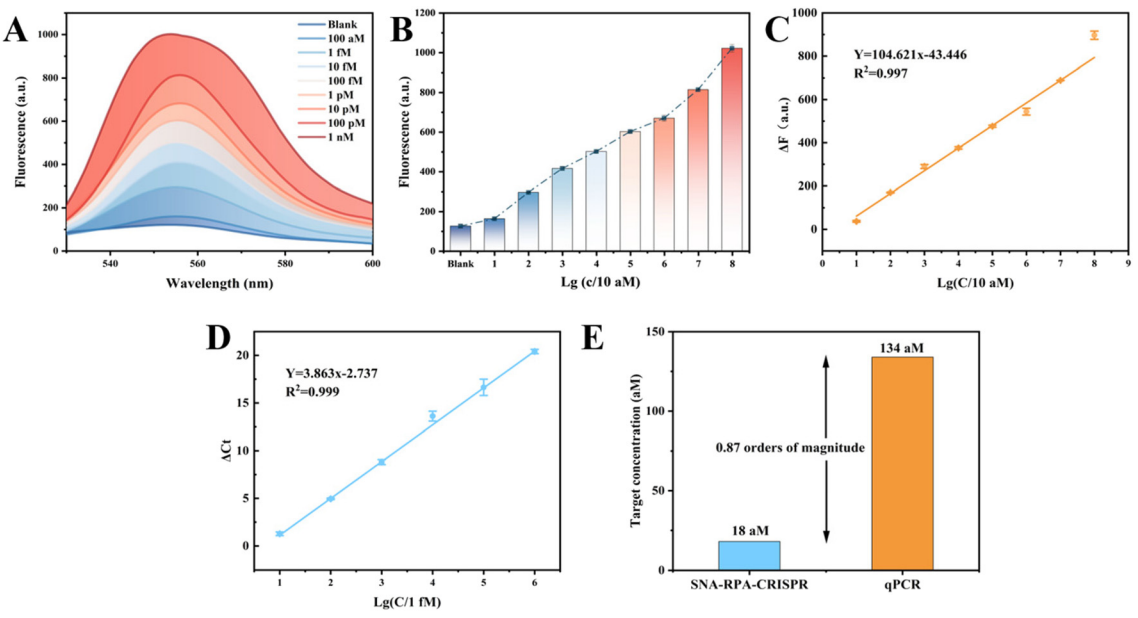

Fig. 3 Sensitivity exploration of the detection of HPV16 dsDNA by SNA-RPA- CRISPR/Cas12a and qPCR. (A) Fluorescence spectra of different concentrations of HPV16 dsDNA detected using SNA-RPA-CRISPR/Cas12a. (B) Fluorescence measurements at 556 nm were performed on HPV16 dsDNA samples of different concentrations using the SNA-RPA-CRISPR assay. (C) Linear relationship between the ΔF and target concentration output by SNA-RPA-CRISPR/Cas12a. (D) Linear relationship between the ΔC_t and target concentration output by SNA-RPA-CRISPR/Cas12a. (E) Comparison of SNA-RPA-CRISPR with qPCR LODs.

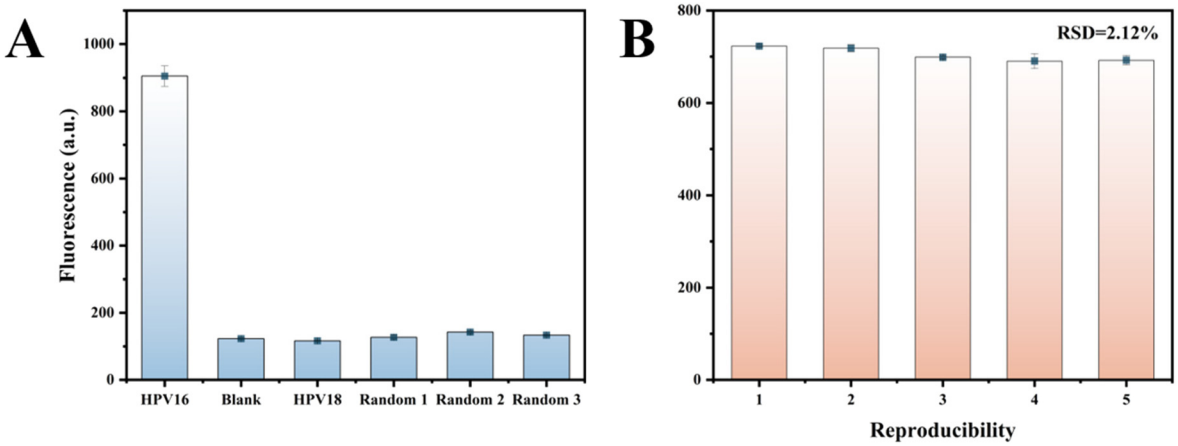

Fig. 4 Specificity (A) and reproducibility (B) of the unpaired SNA-RPA-CRISPR/Cas12a method for HPV16 dsDNA detection explored. All the experiments were conducted in triplicate and graphs are presented as mean ± standard deviation (SD).

Table 1 HPV16 dsDNA spiking assay in 10% human normal serum samples

Serum spiked target concentration	Test results	Recovery rate%	RSD%
10 fM	9.35 fM	93.56	3.72
10 pM	9.51 pM	95.11	0.77
100 pM	107.71 pM	107.71	1.99

using normal serum. The target was diluted with 10% human normal serum into different concentrations: 10 fM, 10 pM, and 100 pM to simulate a complex biological environment. As shown in Table 1 and Fig. S4,† the recoveries of HPV16 dsDNA assay in normal human serum range from 93.56% to 107.71%, with RSDs between 0.77% and 3.72%, indicating that this method can be used to detect HPV16 dsDNA with good stability in complex sample environments.

4 Conclusions

The specific nucleic acid recognition ability of the CRISPR/Cas12a system underpins its important role in biosensing applications. However, when targeting double-stranded DNA (dsDNA), Cas12a activation requires recognition of a protospacer adjacent motif (PAM) site, limiting its application scope since not all target sequences possess a PAM. To overcome this limitation, we developed a semi-nested asymmetric RPA (SNA-RPA) strategy, which generates a large amount of single-stranded DNA (ssDNA) by adjusting primer concentrations and introducing additional primers. The resulting ssDNA can directly hybridize with crRNA and activate Cas12a without the need for PAM recognition.

Using this method, we achieved rapid and highly sensitive detection of HPV16 dsDNA without the addition of extra enzymes or reagents. Targets as low as 18 aM were successfully detected within 70 minutes. This excellent performance is attributed to two key factors: (1) the semi-nested amplification design, where the F2 primer utilizes the F1/R-amplified dsDNA as a template, enabling double verification of the target sequence and producing abundant correct ssDNA, thus significantly enhancing assay specificity; (2) the CRISPR/Cas12a system precisely recognizes the ssDNA guided by crRNA, and its collateral cleavage activity further amplifies the signal, boosting assay sensitivity.

Although the proposed assay demonstrates significant advantages in terms of simplicity, sensitivity, and PAM-independent detection, certain limitations remain to be addressed. Future efforts will focus on integrating this method with intelligent diagnostic devices to enable true point-of-care testing (POCT) and broaden its practical applicability. In addition, further optimization of the amplification strategy to enhance ssDNA yield will be essential for improving assay robustness and ensuring reliable performance across a wider range of clinical settings. Overall, this assay provides a simple, rapid, and cost-effective approach for PAM-independent nucleic acid detection and holds great promise for future clinical applications.

Author contributions

Xiaozhi Zou: conceptualization, methodology, formal analysis, investigation, visualization, and writing – original draft. Tao Gu: visualization and writing – review & editing. Xuheng Li: conceptualization and writing – review & editing. Liyuan Deng: software, formal analysis, and writing – original draft. Shuyu Zhu: software and formal analysis. Jiangbo Dong: investigation and visualization. Fei Deng: writing – original draft. Changjun Hou: funding acquisition, visualization, writing – review & editing, and supervision. Danqun Huo: funding acquisition, writing – review & editing, and supervision.

Conflicts of interest

The authors declare that they have no known competing financial interests or personal relationships that could have appeared to influence the work reported in this paper.

Data availability

All relevant data are within the paper.

Acknowledgements

This work was supported by the National Natural Science Foundation of China (No. 81772290), Graduate Scientific Research and Innovation Foundation of Chongqing, China (CYB240064), Sichuan Province Science and Technology Support Program (2022YFSY0013), Chongqing Graduate Tutor Team Construction Project, and the sharing fund of Chongqing University's large equipment.

References

1 D. Adiga, S. Eswaran, D. Pandey, K. Sharan and S. P. Kabekkodu, *Crit. Rev. Oncol. Hematol.*, 2021, **157**, 103178.
2 S. Ferguson, *Br. Med. J.*, 2024, **386**, q607.
3 N. Izadi, J. Strmiskova, M. Anton, J. Hausnerova and M. Bartosik, *J. Med. Virol.*, 2024, **96**, e70008.
4 M. A. Molina, R. D. M. Steenbergen, A. Pumpe, A. N. Kenyon and W. J. G. Melchers, *Trends Mol. Med.*, 2024, **30**, 890–902.
5 J. Wolf, L. F. Kist, S. B. Pereira, M. A. Quessada, H. Petek, A. Pille, J. G. Maccari, M. P. Mutlaq and L. A. Nasi, *Rev. Med. Virol.*, 2024, **34**, e2537.
6 L. Mirabello, M. Yeager, K. Yu, G. M. Clifford, Y. Xiao, B. Zhu, M. Cullen, J. F. Boland, N. Wentzensen, C. W. Nelson, T. Raine-Bennett, Z. Chen, S. Bass, L. Song, Q. Yang, M. Steinberg, L. Burdett, M. Dean, D. Roberson, J. Mitchell, T. Lorey, S. Franceschi, P. E. Castle, J. Walker, R. Zuna, A. R. Kreimer, D. C. Beachler, A. Hildesheim, P. Gonzalez, C. Porras, R. D. Burk and M. Schiffman, *Cell*, 2017, **170**, 1164–1174.
7 J. M. L. Brotherton, *Lancet Infect. Dis.*, 2017, **17**, 1227–1228.
8 M. Almonte, M. d. l. L. Hernández and P. Adsul, *Lancet Public Health*, 2024, **9**, e838–e839.
9 A. C. Chrysostomou, D. C. Stylianou, A. Constantinidou and L. G. Kostrikis, *Viruses*, 2018, **10**, 729.
10 M. Xu, C. Cao, P. Wu, X. Huang and D. Ma, *Cancer Commun.*, 2024, **45**, 77–109.
11 R. van den Helder, R. D. M. Steenbergen, A. P. van Splunter, C. H. Mom, M. Y. Tjiong, I. Martin, F. M. F. R. Dunné, I. A. M. van der Avoort, M. C. G. Bleeker and N. E. van Trommel, *Clin. Cancer Res.*, 2022, **28**, 2061–2068.
12 X. Wang, X. Deng, Y. Zhang, W. Dong, Q. Rao, Q. Huang, F. Tang, R. Shen, H. Xu, Z. Jin, Y. Tang and D. Du, *Biosens. Bioelectron.*, 2024, **257**, 116268.
13 M. Asif, J. S. Algethami, M. A. M. Alhamami, P. Lie, S. Shaomin and A. Aziz, *Trends Environ. Anal. Chem.*, 2025, **46**, e00263.
14 L. Ma, M. Zhu, Q. Meng, Y. Wang and X. Wang, *Front. Cell. Infect. Microbiol.*, 2024, **13**, 1305222.
15 F. Dai, T. Zhang, F. Pang, T. Jiao, K. Wang, Z. Zhang, N. Wang, Z. Xie, Y. Zhang, Z. Wang, Z. Chen, M. Yu, H. Wei and J. Song, *Biosens. Bioelectron.*, 2025, **270**, 116945.
16 Y. Long, S. Tao, D. Shi, X. Jiang, T. Yu, Y. Long, L. Song and G. Liu, *Aggregate*, 2024, **5**, e569.
17 S. Xing, Z. Lu, Q. Huang, H. Li, Y. Wang, Y. Lai, Y. He, M. Deng and W. Liu, *Theranostics*, 2020, **10**, 10262–10273.
18 M. Wang, W. Chen, M. Li, F. Lin, J. Zhong, W. Ouyang, C. Cai, G. Zeng and H. Liu, *Biosens. Bioelectron.*, 2025, **271**, 117042.
19 X. Li, B. Chen, Y. Xie, Y. Luo, D. Zhu, L. Wang and S. Su, *Anal. Chem.*, 2025, **97**(1), 793–798.
20 H. Li, L. Xiu, X. Guo, Q. Hu and K. Yin, *Chem. Eng. J.*, 2024, **482**, 148872.
21 Y. Ma, H. Wei, Y. Wang, X. Cheng, H. Chen, X. Yang, H. Zhang, Z. Rong and S. Wang, *J. Hazard. Mater.*, 2024, **465**, 133494.
22 M. A. Ahamed, M. A. U. Khalid, M. Dong, A. J. Politza, Z. Zhang, A. Kshirsagar, T. Liu and W. Guan, *Biosens. Bioelectron.*, 2024, **246**, 115866.
23 E. A. Nalefski, R. M. Kooistra, I. Parikh, S. Hedley, K. Rajaraman and D. Madan, *Nucleic Acids Res.*, 2024, **52**, 4502–4522.
24 Z. Duan, X. Zhang, J.-T. Zhang, X. Ji, R. Liu, Y. Chen, S. Li, N. Jia, H. Gao, Y. Xin, N. Jia and J.-K. Zhu, *Cell Res.*, 2025, **35**(2), 145–148.
25 L. Jianwei, C. Jobichen, S. Machida, S. Meng, R. J. Read, C. Hongying, S. Jian, Y. A. Yuan and J. Sivaraman, *PLoS Biol.*, 2023, **21**, e3002023.
26 W. Feng, A. M. Newbigging, J. Tao, Y. Cao, H. Peng, C. Le, J. Wu, B. Pang, J. Li, D. L. Tyrrell, H. Zhang and X. C. Le, *Chem. Sci.*, 2021, **12**, 4683–4698.
27 M. M. Naqvi, L. Lee, O. E. T. Montaguth, F. M. Diffin and M. D. Szczelkun, *Nat. Chem. Biol.*, 2022, **18**, 1014–1022.
28 D. Li, P. Liang, S. Ling, Y. Wu and B. Lv, *Int. J. Biol. Macromol.*, 2024, **266**, 130848.
29 S. Zhou, J. Dong, L. Deng, G. Wang, M. Yang, Y. Wang, D. Huo and C. Hou, *ACS Sens.*, 2022, **7**, 3032–3040.
30 T. Meng, Z. Lin, L. Lu, B. Shao, Y. Luo, Y. Ren, J. Zhang, M. Negahdary, H. Mao, Y. Sun, Y. Wan and F. Song, *Sens. Actuators, B*, 2024, **421**, 136472.
31 G. Cao, N. Yang, Y. Xiong, M. Shi, L. Wang, F. Nie, D. Huo and C. Hou, *ACS Sens.*, 2023, **8**, 4655–4663.
32 X. Wu, G. Liu, Y. Chang, M. Zheng, L. Liu, X. Xia and Y. Feng, *J. Clin. Microbiol.*, 2024, **62**, e0038324.

